JOURNAL OF VIROLOGY, May 2009, p. 4791–4799 Vol. 83, No. 10
0022-538X/09/$08.00+0 doi:10.1128/JVI.02341-08

Herpes Simplex Virus Type 1 Glycoprotein E Mediates Retrograde Spread from Epithelial Cells to Neurites[▽]

Helen M. McGraw and Harvey M. Friedman*

Division of Infectious Diseases, Department of Medicine, University of Pennsylvania School of Medicine, Philadelphia, Pennsylvania 19104-6073

Received 10 November 2008/Accepted 27 February 2009

In animal models of infection, glycoprotein E (gE) is required for efficient herpes simplex virus type 1 (HSV-1) spread from the inoculation site to the cell bodies of innervating neurons (retrograde direction). Retrograde spread in vivo is a multistep process, in that HSV-1 first spreads between epithelial cells at the inoculation site, then infects neurites, and finally travels by retrograde axonal transport to the neuron cell body. To better understand the role of gE in retrograde spread, we used a compartmentalized neuron culture system, in which neurons were infected in the presence or absence of epithelial cells. We found that gE-deleted HSV-1 (NS-gEnull) retained retrograde axonal transport activity when added directly to neurites, in contrast to the retrograde spread defect of this virus in animals. To better mimic the in vivo milieu, we overlaid neurites with epithelial cells prior to infection. In this modified system, virus infects epithelial cells and then spreads to neurites, revealing a 100-fold retrograde spread defect for NS-gEnull. We measured the retrograde spread defect of NS-gEnull from a variety of epithelial cell lines and found that the magnitude of the spread defect from epithelial cells to neurons correlated with epithelial cell plaque size defect, indicating that gE plays a similar role in both types of spread. Therefore, gE-mediated spread between epithelial cells and neurites likely explains the retrograde spread defect of gE-deleted HSV-1 in vivo.

Herpes simplex virus type 1 (HSV-1) is an alphaherpesvirus that characteristically infects skin and mucosal surfaces before spreading to sensory neurons, where it establishes a lifelong persistent infection. The virus periodically returns to the periphery via sensory axons and causes recurrent lesions as well as asymptomatic shedding. This life cycle requires viral transport along axons in two directions: toward the neuron cell body (retrograde direction) and away from the neuron cell body (anterograde direction).

Many studies of alphaherpesvirus neuronal spread have focused on pseudorabies virus (PRV), a virus whose natural host is the pig. Three PRV proteins, glycoprotein E (gE), gI, and Us9, have been shown to mediate anterograde neuronal spread both in animal models of infection and in cultured neurons. However, these three proteins are dispensable for retrograde spread (3, 8, 11, 12, 31, 46). In contrast, numerous animal models of infection have shown that HSV-1 gE is required for retrograde spread from the inoculation site to the cell bodies of innervating neurons (4, 9, 44, 56). In the murine flank model, wild-type (WT) virus replicates in the skin and then infects sensory neurons and spreads in a retrograde direction to the dorsal root ganglia (DRG). In this model, gE-deleted HSV-1 replicates in the skin but is not detected in the DRG (9, 44). This phenotype differs from gE-deleted PRV, which is able to reach the DRG at WT levels (8). Thus, unlike PRV, gE-deleted HSV-1 viruses have a retrograde spread defect in vivo.

HSV-1 gE is a 552-amino-acid type I membrane protein found in the virion membrane as well as in the *trans*-Golgi and plasma membranes of infected cells (1). gE forms a heterodimer with another viral glycoprotein, gI. The gE/gI complex is important for HSV-1 immune evasion through its Fc receptor activity. gE/gI binds to the Fc domain of antibodies directed against other viral proteins, sequestering these antibodies and blocking antibody effector functions (27, 32, 40). Additionally, gE/gI promotes spread between epithelial cells. Viruses lacking either gE or gI form characteristically small plaques in cell culture and small inoculation site lesions in mice (4, 9, 18, 40, 58). In animal models, gE and gI also mediate viral spread in both anterograde and retrograde directions (4, 19, 44, 56).

In order to better understand the role of gE in HSV-1 retrograde neuronal spread, we employed a compartmentalized neuron culture system that has been used to study directional neuronal spread of PRV and West Nile virus (12, 14, 45). In the Campenot chamber system, neurites are contained in a compartment that is separate from their corresponding cell bodies. Therefore, spread in an exclusively retrograde direction can be measured by infecting neurites and detecting spread to neuron cell bodies.

HSV-1 replication requires retrograde transport of incoming viral genomes to the nucleus. In neurites, fusion between viral and cellular membranes occurs at the plasma membrane (43, 48). Upon membrane fusion, the capsid and a subset of tegument proteins (the inner tegument) dissociate from glycoproteins and outer tegument proteins, which remain at the plasma membrane (28, 38). Unenveloped capsids and the associated inner tegument proteins are then transported in the retrograde direction to the nucleus (7, 48, 49).

For both neurons and epithelial cells, retrograde transport is dependent upon microtubules, ATP, the retrograde microtubule motor dynein, and the dynein cofactor dynactin (22, 34,

* Corresponding author. Mailing address: 502 Johnson Pavilion, University of Pennsylvania, Philadelphia, PA 19104-6073. Phone: (215) 662-3557. Fax: (215) 349-5111. E-mail: hfriedma@mail.med.upenn.edu.

▽ Published ahead of print on 11 March 2009.

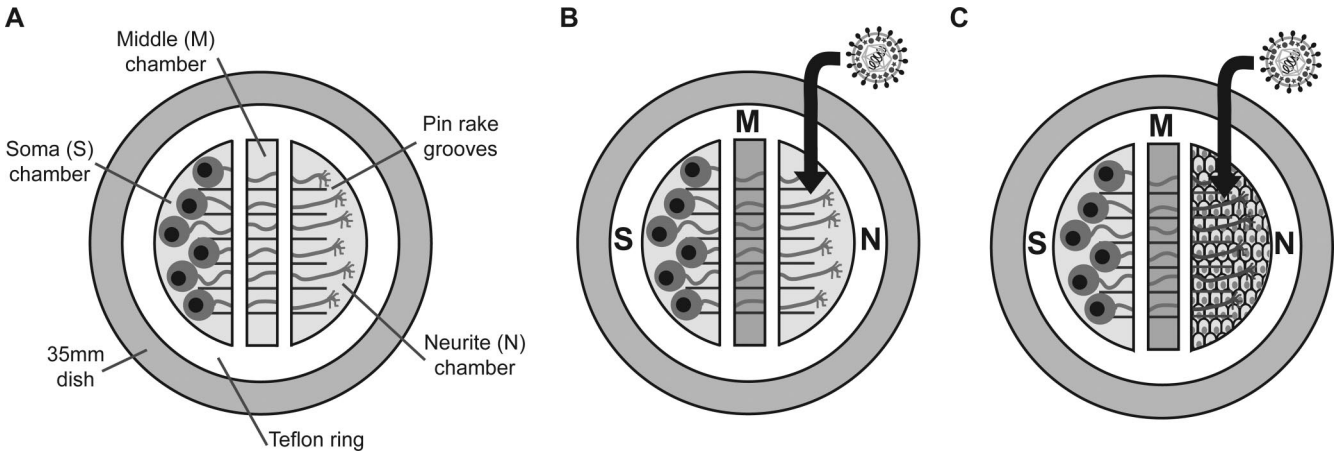

FIG. 1. Campenot culture system. (A) Campenot chambers consist of a Teflon ring which divides the culture into three separate compartments. Neurons are seeded into the S chamber and extend their axons along pin rake grooves into the M and N chambers. (B and C) The M chamber is filled with 1% methylcellulose prior to infection. Virus is added to the N chamber neurites either directly (B) or via overlaid epithelial cells (C).

49, 52). Several viral proteins interact with components of the dynein motor complex (23, 39, 60). However, none of these proteins suggest a completely satisfactory mechanism by which viral retrograde transport occurs, either because they are not components of the complex that is transported to the nucleus (UL34, UL9, VP11/12) or because capsids lacking that protein retain retrograde transport activity (VP26) (2, 17, 21, 28, 37). This implies that additional viral proteins are involved in retrograde trafficking.

We sought to better characterize the role of gE in retrograde spread and found that gE is dispensable for retrograde axonal transport; however, it promotes HSV-1 spread from epithelial cells to neurites. This epithelial cell-to-neuron spread defect provides a plausible explanation for the retrograde spread defect of gE-deleted HSV-1 in animal models of infection.

MATERIALS AND METHODS

Cells. Vero cells (African green monkey kidney epithelial cells), HEp-2 cells (human epidermoid laryngeal carcinoma cells), 293T cells (human kidney epithelial cells), HaCaT cells (human keratinocytes), and L cells (murine fibroblasts) were propagated in Dulbecco's modified Eagle medium (DMEM) supplemented with 10 mM HEPES (pH 7.3), 2 mM L-glutamine, 20 μg/ml gentamicin, and 5% heat-inactivated fetal bovine serum. HEC-1-A cells (human endometrial adenocarcinoma cells) were propagated in McCoy's 5A medium supplemented with 10% fetal bovine serum, 2 mM L-glutamine, and 100 U/ml penicillin-streptomycin. Unless otherwise indicated, HaCaT and HEC-1-A cells were allowed to grow for 1 week before infection, during which time they acquired morphologies consistent with polarization.

Viruses. HSV-1 strain NS is a low-passage clinical isolate used as the WT strain for these studies. NS-gEnull contains an ICP6::LacZ expression cassette, replacing gE amino acids 124 to 510, and produces no functional gE protein (40). A rescued virus, rNS-gEnull, was prepared by cotransfection of NS-gEnull viral DNA and a gE-encoding plasmid and selection of gE-positive plaques (40). Virus stocks were prepared by infecting Vero cells at a multiplicity of infection (MOI) of 0.01 and collecting the infected cells and media when the cytopathic effect reached 100%. Virions were pelleted from the clarified supernatant and purified on a 10%-30%-60% sucrose step gradient. Purified virions were pelleted at 112,000 × *g* and resuspended in phosphate-buffered saline (PBS). For some experiments, viral stocks were prepared with L cells instead of Vero cells.

Plaque assay. Viral titers were determined by plaque assay. Vero cells were washed twice with PBS and infected in triplicate with 150 μl of virus in DMEM. Cells were incubated for 1 h at 37°C, washed twice with PBS, and overlaid with medium containing 0.6% low-melt agarose. Plaques were counted at 40× magnification at 2 days postinfection (dpi).

SCG neuron culture. Superior cervical ganglia (SCG) were dissected from E17 Sprague-Dawley rat embryos (Charles River Laboratories). The dissociated ganglia were plated on tissue culture dishes (Falcon) coated with 500 μg poly-DL-ornithine hydrobromide (Sigma) and 10 μg natural mouse laminin (Invitrogen) (13). The neurons were cultured in medium consisting of 10 mg/ml bovine serum albumin dissolved in a 1:1 dilution mixture of DMEM and Ham's F12 nutrient mixture (Gibco). The medium was supplemented with 4.6 mg/ml glucose, 2 mM L-glutamine, 16 μg/ml putrescine (Sigma), 100 μg/ml holo-transferrin (Sigma), 10 μg/ml insulin (Sigma), 50 U/ml penicillin-streptomycin, 100 ng/ml nerve growth factor (Promega), 30 nM selenium (Sigma), and 20 nM progesterone (Sigma). Two days after being plated, the cultures were treated for 24 h with 1 μM cytosine-1-β-D-arabinofuranoside, a mitotic inhibitor. The culture medium was changed every 3 to 4 days.

Campenot chamber system. SCG neurons were cultured in Campenot chambers, as previously described (10, 12). Campenot chambers consist of a three-part Teflon ring that divides the culture into soma (S), middle (M), and neurite (N) compartments (Fig. 1A). A pin rake was used to scratch parallel grooves onto coated dishes. Prior to chamber assembly, a drop of 1% methylcellulose was applied to the scratches to ensure a moist seal that would permit axon penetration. CAMP320 Teflon chambers were purchased from Tyler Research (Edmonton, Alberta, Canada). The chambers were held to the dishes using silicone grease (Dow Corning) that was applied along the septum and circumference of the chamber. Dissociated neurons from half of an SCG (resulting in approximately 5,000 neuron cell bodies) were seeded into the S chamber and cultured for 2 to 3 weeks until extensive neurite growth was observed in the N chamber (12). For some experiments, epithelial cells were seeded over N chamber neurites. All epithelial cells were seeded at a density to produce a confluent monolayer the following day. HEC-1-A cells were allowed to grow for 1 week prior to infection, whereas Vero, HEp-2, and 293T cells were infected 1 day after being seeded. For some experiments, HaCaT cells were grown for 1 week prior to infection, while for others, they were infected 1 day after being seeded. When epithelial cells were cocultured with neurites, a 1:1 dilution mixture of neuron medium-epithelial cell medium was used in the N chamber.

Infection of neurons in Campenot chambers. One day prior to infection, the culture medium was changed, and the M chamber was filled with neuron medium containing 1% methylcellulose. The culture medium in the N chamber was replaced by 50 μl of viral inoculum in neuron medium. After 1 h at 37°C, the inoculum was removed. For experiments evaluating direct infection of neurites (Fig. 1B), the N chamber was then filled with culture medium. For experiments evaluating spread of infection from epithelial cells to neurons (Fig. 1C), the N chamber was filled with a 1:1 dilution mixture of neuron medium-epithelial cell medium containing 1% methylcellulose. At the times indicated in the figures, the contents of the N and S chambers were collected using a pipette tip to harvest the cells and medium together, and the samples were stored at −80°C. The NS-gEnull retrograde spread defect was calculated as the difference between the log-transformed S chamber titers of NS and NS-gEnull.

Single-step growth curves. Dissociated neurons from half of an SCG were infected with 2.5×10^5 PFU NS or NS-gEnull. This high-input titer was required

to ensure the infection of all neurons in the culture, since many virions adhere to the culture matrix rather than to the neurons (47). Following 1 h of incubation, the neurons were acid washed with citrate buffer, pH 3.0, for 1 min to inactivate extracellular virus. The neurons were washed twice with PBS, and then neuron medium was added. At 1 to 24 hpi, the cells and medium were harvested together and stored at −80°C. HaCaT or HEp-2 cells were infected with NS or NS-gEnull at an MOI of 5 and acid washed after 1 h. Cells and media were harvested separately and stored at −80°C. All samples were sonicated prior to being titered on Vero cells.

Plaque size determination. Confluent epithelial cells were infected with HSV-1 NS or NS-gEnull at approximately 50 PFU/well to obtain well-separated plaques. Infected cells were overlaid with 0.6% low-melt agarose. The overlay was removed at 2 or 4 dpi, and cells were fixed with a 1:1 dilution of methanol-acetone. Plaques were stained using rabbit anti-HSV-1 (Dako), horseradish peroxidase-conjugated secondary antibody (Amersham), and 3,3′-diaminobenzidine tetrahydrochloride (DAB) substrate (Sigma). Plaques were measured with a micrometer at 40× magnification, and the area was calculated from two perpendicular diameters. The average area was determined by measuring 25 plaques in each of the two experiments. The NS-gEnull plaque size defect was defined as the area of NS-gEnull plaques expressed as a percentage of the NS plaque area.

Statistical analysis. Statistical analysis was performed with GraphPad Prism software. All statistical comparisons were between NS and NS-gEnull.

RESULTS

Growth curves. We performed experiments to obtain single-step growth curves to compare the replication of HSV-1 NS and NS-gEnull in neurons and epithelial cells. In dissociated SCG neurons, NS and NS-gEnull had similar replication kinetics and yields (Fig. 2A). NS and NS-gEnull also displayed comparable single-step growth curves in HaCaT and HEp-2 cells (Fig. 2B and C). Therefore, gE is not required for replication in neurons or in polarized (HaCaT) or nonpolarized (HEp-2) epithelial cells.

Retrograde spread from neurites. SCG neurons grown in Campenot chambers were used to measure HSV-1 retrograde axonal transport. A total of 1×10^5 PFU HSV-1 NS or NS-gEnull was added to the N chamber (Fig. 1B), and the contents of the S chamber were titered at 12, 18, or 24 hpi. At all time points, comparable titers of NS and NS-gEnull were detected in the S chamber (Fig. 3). When the input dose was increased 10-fold to 1×10^6 PFU, NS and NS-gEnull still produced equivalent titers in the S chamber (data not shown). These results indicate that NS-gEnull retains retrograde axonal transport activity in vitro, which is in contrast to the retrograde spread defect observed in animals.

Virus stocks prepared in murine L cells. In the Campenot chamber system, neurites were infected with virus that was propagated in Vero (primate) cells. However, in the murine flank model, HSV-1 first replicates in epithelial cells before spreading to neurites; therefore, neurons are infected by virus produced in murine cells (40). We compared retrograde axonal transport of NS and NS-gEnull viruses prepared in Vero or L cells to determine whether differences in neuron infection are dependent on the cell type used to prepare virus stocks. Virus was added to neurites in the N chamber, and the contents of the S chamber were titered at 18 hpi. NS and NS-gEnull produced equivalent S chamber titers, regardless of whether the virus was grown in Vero or L cells (Fig. 4). Thus, viral replication in murine cells does not explain the NS-gEnull retrograde spread defect observed with animal models.

Retrograde spread from polarized epithelial cells. gE promotes epithelial cell-to-cell spread; therefore, we postulated

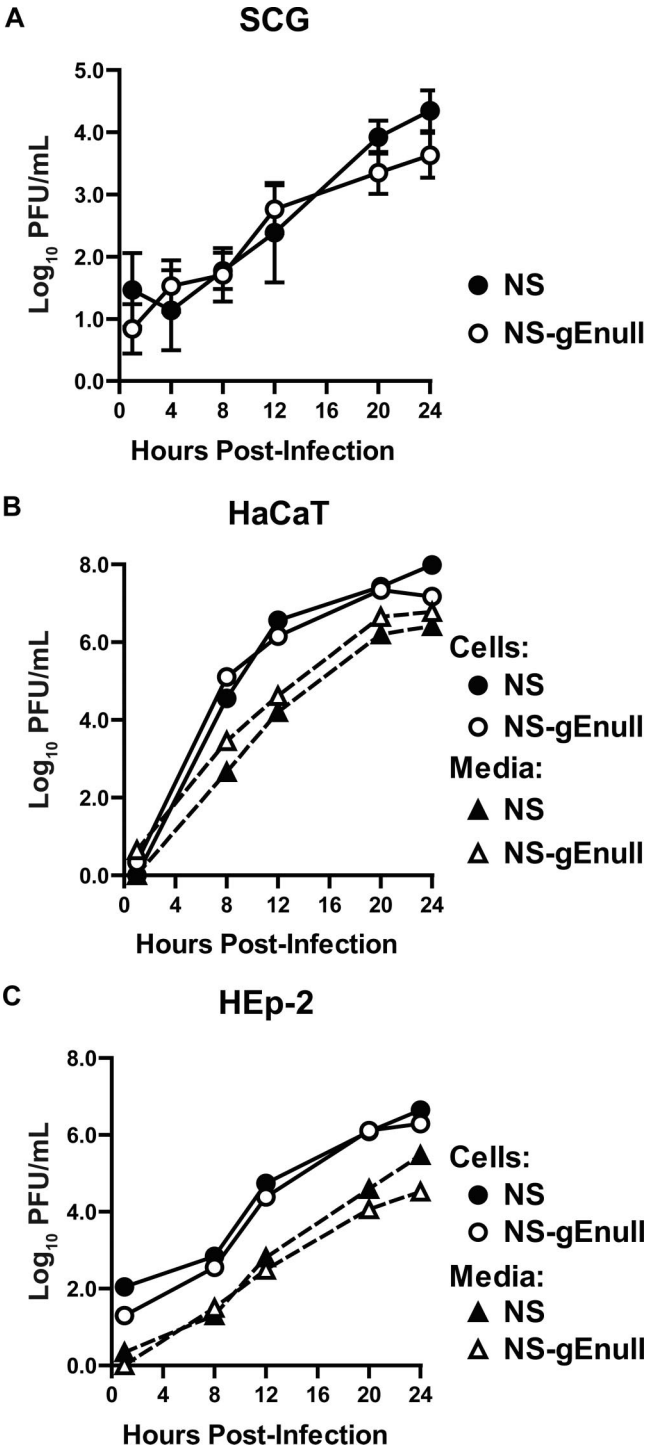

FIG. 2. Replication in neurons and epithelial cells. (A) Dissociated SCG neurons were infected with 2.5×10^5 PFU HSV-1 NS or NS-gEnull. Cells and media were titered together on Vero cells. Results shown are the means ± standard errors of four experiments. (B and C) Polarized HaCaT cells (B) and HEp-2 cells (C) were infected with HSV-1 NS or NS-gEnull at an MOI of 5. Cells and media were collected separately and titered on Vero cells. The results from one experiment are shown.

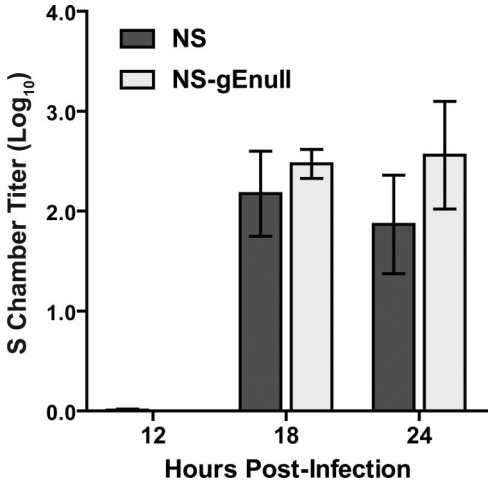

FIG. 3. gE is dispensable for retrograde axonal transport. SCG neurons were grown in Campenot chambers, and N chamber neurites were infected with 1×10^5 PFU HSV-1 NS or NS-gEnull. Cells and media from the S chamber were collected together and titered on Vero cells. Results shown are the means ± standard errors from three to six chambers. *P* was >0.05 at all time points.

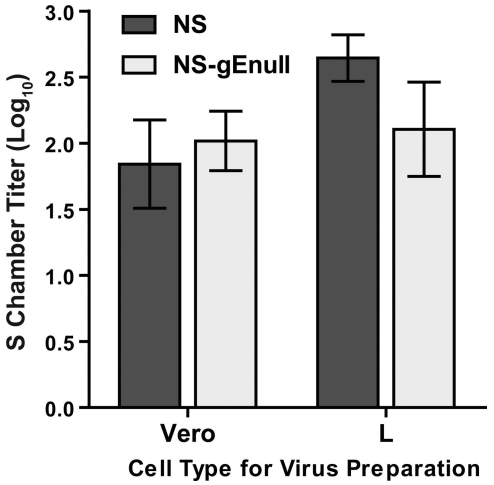

FIG. 4. NS-gEnull grown in murine L cells retains retrograde axonal transport activity. SCG neurons were grown in Campenot chambers, and N chamber neurites were infected with 1×10^5 PFU HSV-1 NS or NS-gEnull that had been propagated in either Vero or L cells. Cells and media from the S chamber were collected together and titered on Vero cells at 18 hpi. Results shown are the means ± standard errors from five to six chambers. *P* was >0.05 for both cell types.

that gE may mediate spread between epithelial cells and neurons. The Campenot culture system was modified to allow HSV-1 to spread to neurites from infected epithelial cells (Fig. 1C), rather than allowing virus to infect the neurites directly. Once neurites had penetrated into the N chamber (approximately 1 to 2 weeks in culture), HaCaT cells were seeded on top of the neurites and grown for 1 week before infection. After 1 week in culture, HaCaT cells remain as an intact monolayer and acquire a morphology consistent with polarization. The N chamber was infected with 1×10^5 PFU HSV-1 NS, rNS-gEnull, or NS-gEnull, which represents an MOI of 1 PFU/HaCaT cell. One hour following infection, the N chamber was filled with media containing 1% methylcellulose to restrict cell-free virus spread. The contents of the N and S chambers were titered at 24, 36, 48, and 72 hpi. At each time point, NS and NS-gEnull produced equivalent titers in the N chamber (Fig. 5A), indicating that the amounts of virus available to infect neurites were comparable. Despite equivalent N chamber titers, NS-gEnull was detected in only one of eight S chambers at 24 hpi, and the S chamber titers were significantly lower than those of NS at 36, 48, and 72 hpi (Fig. 5B). The rescued virus, rNS-gEnull, fully restored the retrograde spread defect of NS-gEnull (Fig. 5B). NS-gEnull retained retrograde spread activity when the N chamber was overlaid with methylcellulose following direct neurite infection (data not shown), indicating that the methylcellulose overlay was not responsible for the spread defect. We conclude that gE is required for efficient spread between epithelial cells and neurites, since NS-gEnull had a retrograde spread defect when added to HaCaT cells but not when the virus was added directly to neurites.

Retrograde spread at various input doses. To quantify the NS-gEnull spread defect, we evaluated retrograde spread from HaCaT cells to neurites at a range of input doses. A dose of 1×10^4, 1×10^5, or 1×10^6 PFU HSV-1 NS or NS-gEnull was added to HaCaT cells in the N chamber, and the N and S chambers were titered at 36 hpi. NS and NS-gEnull produced comparable titers in the N chamber at all three input doses (data not shown), yet differences in the S chamber were detected. At a 1×10^4 PFU input dose, the NS S chamber titer was 3 PFU/chamber, and no NS-gEnull was detected, while at 1×10^5 and 1×10^6 PFU, NS-gEnull titers were significantly lower than those of NS (Fig. 6). A total of 1×10^6 PFU of NS-gEnull produced approximately the same S chamber titers as infection with 2 $\log_{10}$-lower titers of NS. The S chamber titers produced by 1×10^5 PFU NS-gEnull were also approximately 2 $\log_{10}$ lower than those produced by NS at the same input dose. Therefore, NS-gEnull is impaired approximately 100-fold at spread between epithelial cells and neurites.

Retrograde spread from various epithelial cell types. Previous work showed that gE promotes basolateral targeting of HSV-1 in polarized (HEC-1-A and HaCaT) cells but that gE is dispensable for targeting of HSV-1 in nonpolarized (HEp-2) cells (24, 33). Therefore, we compared retrograde spread of NS and NS-gEnull from polarized and nonpolarized HaCaT cells in the Campenot culture system. HaCaT cells were seeded on top of N chamber neurites and either were grown for 1 week prior to infection to allow the cells to polarize or were infected the following day, prior to polarization. A total of 1×10^5 PFU HSV-1 NS or NS-gEnull was added to the N chamber, and the contents of the S chamber were titered at 36 hpi. No significant differences were detected between NS and NS-gEnull N chamber titers for either the 1-week-old or 1-day-old HaCaT cells (data not shown). Although NS-gEnull S chamber titers were lower than those of NS for both 1-week-old and 1-day-old HaCaT cells, the retrograde spread defect was much more pronounced for 1-week-old HaCaT cells (Fig. 7A). Thus, NS-gEnull has a greater retrograde spread defect from polarized than from nonpolarized HaCaT cells, consistent with the known role of gE in basolateral targeting.

To extend these observations to additional epithelial cell lines, HEC-1-A cells (a polarized cell type) or Vero, HEp-2, or

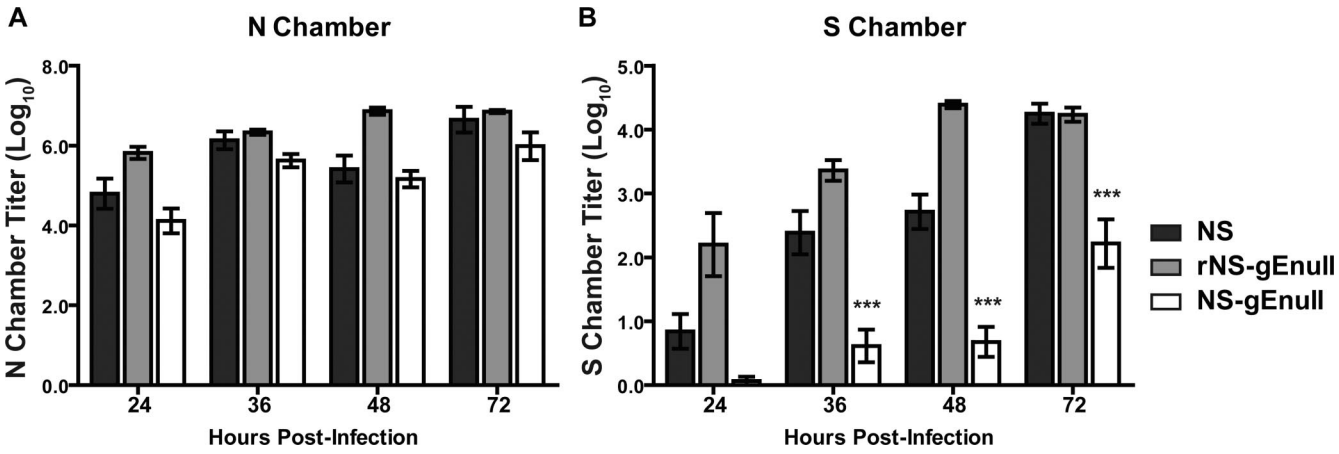

FIG. 5. HSV-1 gE promotes spread between HaCaT cells and neurites. HaCaT cells were seeded on top of N chamber neurites and grown for 1 week, during which time they acquired a polarized morphology. The N chamber was infected with 1×10^5 PFU HSV-1 NS, rNS-gEnull, or NS-gEnull and overlaid with 1% methylcellulose. The contents of the N (A) and S (B) chambers were titered on Vero cells. Results shown are the means ± standard errors of 3 to 10 chambers. Statistical comparisons are between NS and NS-gEnull. N chamber, P of >0.05 at all time points. ***, P of <0.001.

293T cells (nonpolarized cell types) were seeded on top of the N chamber neurites (5, 6, 15, 29). HEC-1-A cells were allowed to polarize for 1 week prior to infection, while other cell types were infected 1 day after being seeded into the N chamber. A total of 1×10^5 PFU HSV-1 NS or NS-gEnull was added to the N chamber, and the contents of the S chambers were titered at 36 hpi. No significant differences were detected between NS and NS-gEnull N chamber titers in any cell type (data not shown). NS-gEnull produced lower S chamber titers than NS in all cell types (Fig. 7B), although the retrograde spread defects of NS-gEnull in these cell types were intermediate compared to those observed with 1-week-old and 1-day-old HaCaT cells. Similar retrograde spread defects were observed when epithelial cells were infected with 1×10^6 PFU (data not shown). These results indicate that gE is important for HSV-1 spread to neurites from a variety of epithelial cell types but that the effect is most pronounced for polarized cells.

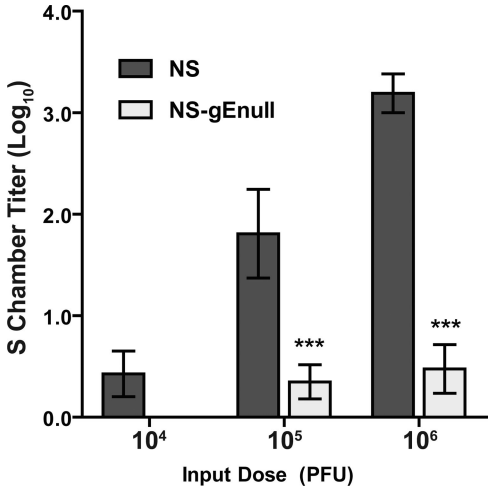

FIG. 6. NS-gEnull is impaired 100-fold at retrograde spread from HaCaT cells to neurites. HaCaT cells were seeded on top of N chamber neurites and allowed to polarize for 1 week. A dose of 1×10^4, 1×10^5, or 1×10^6 PFU HSV-1 NS or NS-gEnull was added to the N chamber, which was overlaid with 1% methylcellulose following infection. The contents of the S chamber were titered at 36 hpi. Results shown are the means ± standard errors of six to seven chambers. ***, P of <0.001.

Plaque size. gE promotes spread between epithelial cells, as indicated by the small plaques produced by gE-deleted viruses in culture (4, 18, 58). As this phenotype has been described mainly for polarized epithelial cells, we compared NS and NS-gEnull plaque sizes for several polarized and nonpolarized cell types. At 2 dpi, NS-gEnull produced smaller plaques than NS in all cell types, with significant differences observed for HaCaT cells grown for 1 week or 1 day prior to infection and for Vero cells (Fig. 8A). Since both viruses produced very small plaques in HEC-1-A, HEp-2, and 293T cells, plaques were also measured at 4 dpi for these cell types (Fig. 8B). NS-gEnull plaques were significantly smaller than those of NS in 293T cells at 4 dpi. In all three cell types, plaques were larger at 4 dpi, but the relative size of NS-gEnull plaques compared to those of NS was similar at 2 and 4 dpi.

To determine if plaque size defects correlate with retrograde spread defects, we compared the difference between NS and NS-gEnull S chamber titers with the relative plaque size for each cell type. For HaCaT and Vero cells, the plaque size at 2 dpi was used in the correlation, while the plaque size at 4 dpi was used for HEC-1-A, 293T, and HEp-2 cells. A significant correlation between plaque size and retrograde spread was detected (Fig. 8C), suggesting that gE mediates spread both between epithelial cells and from epithelial cells to neurites.

DISCUSSION

We used a compartmentalized neuron culture system to study the role of gE in HSV-1 retrograde spread. While NS-gEnull retained retrograde axonal transport activity, it was defective at retrograde spread from epithelial cells to neuron cell bodies. We postulate that this epithelial cell-to-neuron spread defect accounts for the retrograde spread defect observed with gE-deleted HSV-1 in animal models.

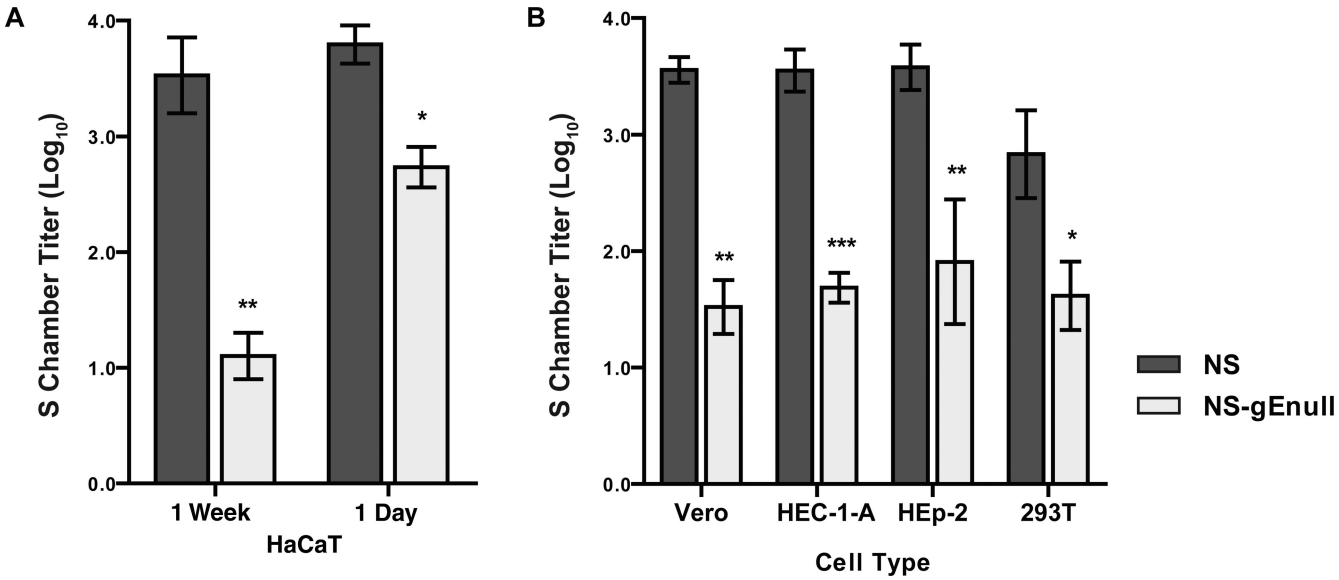

FIG. 7. HSV-1 gE promotes spread between various epithelial cell types and neurites. (A) HaCaT cells were seeded on top of N chamber neurites and infected either 1 week or 1 day later with 1×10^5 PFU HSV-1 NS or NS-gEnull. The contents of the S chamber were titered 36 hpi. (B) Vero, HEp-2, or 293T cells were seeded on top of N chamber neurites and infected with 1×10^5 PFU HSV-1 NS or NS-gEnull the following day, while HEC-1-A cells were infected after 1 week. The contents of the S chamber were titered at 36 hpi. Results shown are the means ± standard errors for three to seven chambers. ***, P of <0.001; **, P of <0.001; *, P of <0.05.

Retrograde spread of gE-deleted HSV-1 has been assessed with at least four animal models. In all cases, the gE-deleted virus showed a pronounced defect in spread from the inoculation site to the cell bodies of innervating neurons. In the murine flank model, NS-gEnull was inoculated onto the skin, and no virus was detected in the DRG by titering or quantitative PCR (9, 44). In the murine retina model, NS-gEnull was injected into the vitreous body of the eye, and no viral antigens were detected at brain sites reached by retrograde spread from the eye (56). After inoculation onto the ear pinna, HSV-1 gEnull (strain SC16) was greatly impaired at spread to the innervating sensory ganglia, although low titers of virus were detected (4). When mice were infected with NS-gEnull by corneal scarification, genome copies in the trigeminal ganglia were greatly reduced compared to those infected with HSV-1 NS (H. Friedman, unpublished observation). One possible explanation for this phenotype is that NS-gEnull spreads to innervating ganglia but replicates inefficiently, resulting in lower viral titers and fewer genome copies. This explanation seems unlikely, since we demonstrated that NS-gEnull replicates with WT kinetics and produces WT yields in cultured neurons, which is consistent with observations by others (19).

In vivo spread of gE-deleted HSV-1 to secondary tissues is influenced by reduced epithelial cell-to-cell spread at the inoculation site, resulting in lower titers available to infect neurons (4, 9, 18). Therefore, we used a compartmentalized neuron culture system to directly study retrograde spread of HSV-1. With this system, the input titer of virus can be adjusted to minimize the effect of epithelial cell-to-epithelial cell spread on neurite infection.

We showed that when NS-gEnull was added directly to neurites, it had no defect in retrograde spread, which is in marked contrast to the phenotype of this virus in animal models. There are several characteristics that differ between the Campenot system and animal models of HSV-1 spread. We used rat sympathetic neurons in these experiments because their robust axon growth allows them to penetrate the silicone grease barrier separating the S, M, and N chambers. In contrast, HSV-1 preferentially infects sensory neurons in mouse models, although retrograde spread along parasympathetic and motor neurons is observed in the mouse retina model of infection (56). More importantly, however, in animal models, HSV-1 first replicates in epithelial cells and then spreads to innervating neurons. To better mimic the in vivo milieu, we seeded polarized epithelial cells (HaCaT cells) on top of neurites. The time course of infection indicates that the epithelial cells largely prevented direct infection of neurites. This conclusion is based on the observation that NS was readily detected in the S chamber at 18 h following direct infection of neurites, while it took 36 h to reach comparable S chamber titers in the presence of HaCaT cells, indicating that the virus replicated first in HaCaT cells before infecting neurites.

In the presence of HaCaT cells, NS-gEnull had a 100-fold deficit in retrograde spread to the S chamber. The NS-gEnull retrograde spread defect in vivo is more pronounced than in Campenot chambers (9, 44, 56). It is unlikely that a single monolayer of HaCaT cells provides as large a barrier to neurite infection as do the multiple layers of epithelial cells present in skin. In addition, free neurites are likely exposed along the pin rake grooves in the N chamber, as epithelial cells adhere poorly at these sites, facilitating direct infection of neurites. Even in animals, direct infection of neurons may occur occasionally. When mice were inoculated intranasally with *dl*5-29, a replication-defective HSV-1 vaccine strain, low levels of viral DNA were detected in the trigeminal ganglia of some mice (16). Since this virus is replication defective, viral DNA in the ganglia indicates that neurons were directly infected by the virus. Interestingly, no *dl*5-29 DNA was detected in the ganglia

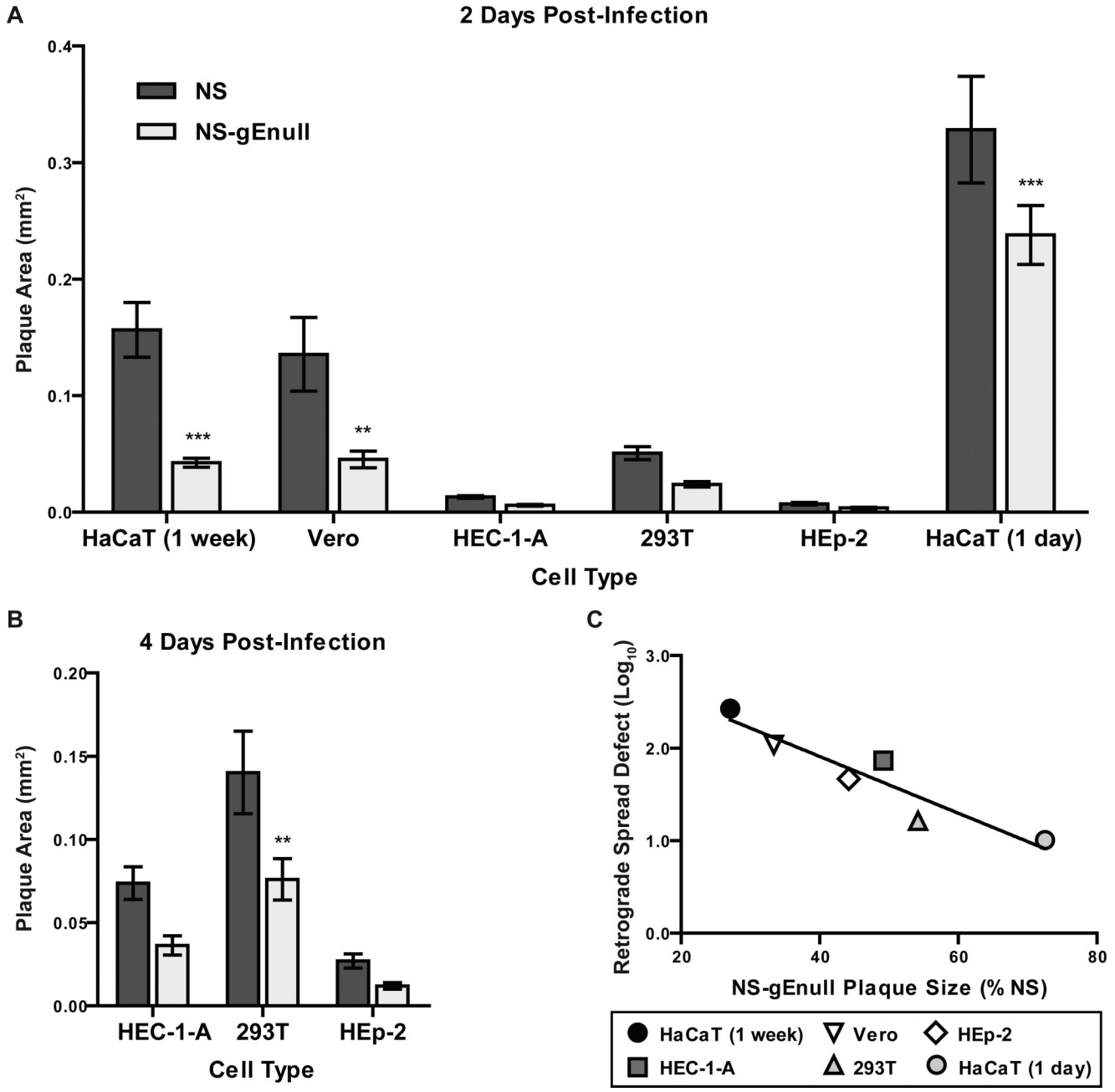

FIG. 8. The NS-gEnull plaque size defect correlates with its retrograde spread defect. (A and B) Epithelial cells were infected with approximately 50 PFU/well of HSV-1 NS or NS-gEnull and overlaid with agarose. Plaque size was measured at 2 (A) or 4 (B) dpi. ***, P of <0.001; **, P of <0.01; *, P of <0.05. (C) The NS-gEnull plaque size defect was plotted versus the NS-gEnull retrograde spread defect. R^2, 0.866; P, 0.007.

after intradermal or intramuscular inoculation, which may indicate that free neurites are more accessible to HSV-1 at particular anatomic sites. HSV-1 commonly infects richly innervated mucosal surfaces, such as oral or vaginal mucosa, that are protected only by a thin epithelial layer, which may leave neurites more accessible to infection. The accessibility of free neurites at certain anatomic sites may explain the variation in retrograde spread defects observed with different animal models after infection with gE-deleted HSV-1.

Interestingly, gE-deleted PRV and bovine herpesvirus 1 (BHV-1) retain retrograde spread activity in animals, although these viruses produce small plaques in culture (3, 8, 11, 31, 35, 46, 51, 53–55). These findings may indicate that PRV and BHV-1 rely less on gE for epithelial cell-to-neuron spread than does HSV-1. PRV cell-to-cell spread does not require the receptor binding protein gD, whereas HSV-1 and BHV-1 spread is gD dependent, indicating that these related alphaherpesviruses have different molecular requirements for cell-to-cell spread (26, 36, 42).

The cell-to-cell spread defects of HSV-1 gE mutants have

been reported mainly for polarized cell types (25, 30, 41, 59). In an electron microscopy study, WT virions localized to the basolateral surface of polarized HEC-1-A and HaCaT cells, whereas gE-deleted virions localized to the apical surface (24, 33). In contrast, no localization difference was observed between the gE-deleted and WT viruses in nonpolarized HEp-2 cells (33). These observations suggested that the role of gE in cell-to-cell spread is most apparent in polarized cell types. Our results comparing 1-week-old and 1-day-old HaCaT cells support the conclusion that gE is more important for spread from polarized cells than from nonpolarized cells.

Although NS-gEnull was impaired at epithelial cell-to-epithelial cell spread (plaque size) and epithelial cell-to-neurite spread (retrograde spread) in all cell types tested, the spread defects tended to be greater in polarized cell types than in nonpolarized ones. An exception was Vero cells, which are nonpolarized but had a more pronounced plaque size and spread phenotype than polarized HEC-1-A cells (5, 29). Interestingly, HSV-1 assembly compartments have been observed on the basal surface of Vero cells, suggesting that assembly and egress may be targeted to a specific cell surface even in nonpolarized epithelial cells (50).

Although the Campenot system is not compatible with standard methods for verifying epithelial cell polarization, three lines of reasoning suggest that HaCaT cells grown for 1 week in this system are, in fact, polarized. First, HaCaT cells grown on laminin-coated Transwell filters have been shown to polarize, as measured by inulin impermeability (57). In the Campenot system, HaCaT cells are also grown on a laminin substrate. Second, NS-gEnull has a greater defect in epithelial cell-to-neurite spread from HaCaT cells grown for 1 week before infection than from cells grown for 1 day, suggesting that the cells undergo changes during this time period. Third, in contrast to HaCaT and HEC-1-A cells, which maintained confluent monolayers susceptible to HSV-1 infection after 1 week in culture, HEp-2 cells grown for 1 week under identical conditions piled up, appeared unhealthy, and were largely refractory to HSV-1 infection (data not shown). Thus, unlike HaCaT cells, HEp-2 cells, which fail to polarize, are unable to maintain an intact monolayer for a sustained period of time. These observations support the conclusion that HaCaT cells are polarized after 1 week in the N chamber.

HSV-1 gE likely mediates cell-to-cell spread by multiple molecular mechanisms. Mutations in either the cytoplasmic tail or ectodomain of gE can produce a small plaque phenotype equivalent to that of gE-deleted viruses (25, 41, 44). The cytoplasmic tail of gE contains tyrosine-signaling motifs that are required to target virions to cell junctions, the sites of cell-to-cell spread (25, 33, 59). The gE ectodomain also promotes efficient cell-to-cell spread, possibly by interacting with an unidentified ligand at cell junctions (20, 41). The relative roles of the gE cytoplasmic tail and ectodomain in epithelial cell-to-neuron spread cannot be determined from the studies reported here, as NS-gEnull lacks both gE domains. Further studies are required to define the domains of gE involved in epithelial cell-to-neuron spread.

ACKNOWLEDGMENTS

This work was supported by NIH grant AI33063.

We thank members of the Enquist laboratory for their assistance with SCG culture and Campenot chamber techniques.

REFERENCES

1. **Alconada, A., U. Bauer, B. Sodeik, and B. Hoflack.** 1999. Intracellular traffic of herpes simplex virus glycoprotein gE: characterization of the sorting signals required for its *trans*-Golgi network localization. J. Virol. **73:**377–387.
2. **Antinone, S. E., G. T. Shubeita, K. E. Coller, J. I. Lee, S. Haverlock-Moyns, S. P. Gross, and G. A. Smith.** 2006. The herpesvirus capsid surface protein, VP26, and the majority of the tegument proteins are dispensable for capsid transport toward the nucleus. J. Virol. **80:**5494–5498.
3. **Babic, N., B. Klupp, A. Brack, T. C. Mettenleiter, G. Ugolini, and A. Flamand.** 1996. Deletion of glycoprotein gE reduces the propagation of pseudorabies virus in the nervous system of mice after intranasal inoculation. Virology **219:**279–284.
4. **Balan, P., N. Davis-Poynter, S. Bell, H. Atkinson, H. Browne, and T. Minson.** 1994. An analysis of the in vitro and in vivo phenotypes of mutants of herpes simplex virus type 1 lacking glycoproteins gG, gE, gI or the putative gJ. J. Gen. Virol. **75:**1245–1258.
5. **Ball, J. M., Z. Moldoveanu, L. R. Melsen, P. A. Kozlowski, S. Jackson, M. J. Mulligan, J. F. Mestecky, and R. W. Compans.** 1995. A polarized human endometrial cell line that binds and transports polymeric IgA. In Vitro Cell. Dev. Biol. Anim. **31:**196–206.
6. **Batonick, M., A. G. Oomens, and G. W. Wertz.** 2008. Human respiratory syncytial virus glycoproteins are not required for apical targeting and release from polarized epithelial cells. J. Virol. **82:**8664–8672.
7. **Bearer, E. L., X. O. Breakefield, D. Schuback, T. S. Reese, and J. H. LaVail.** 2000. Retrograde axonal transport of herpes simplex virus: evidence for a single mechanism and a role for tegument. Proc. Natl. Acad. Sci. USA **97:**8146–8150.
8. **Brittle, E. E., A. E. Reynolds, and L. W. Enquist.** 2004. Two modes of pseudorabies virus neuroinvasion and lethality in mice. J. Virol. **78:**12951–12963.
9. **Brittle, E. E., F. Wang, J. M. Lubinski, R. M. Bunte, and H. M. Friedman.** 2008. A replication-competent, neuronal spread-defective, live attenuated herpes simplex virus type 1 vaccine. J. Virol. **82:**8431–8441.
10. **Campenot, R. B.** 1992. Compartmented culture analysis of nerve growth, p. 275–298. *In* B. Stevenson, D. Paul, and W. Gallin (ed.), Cell-cell interactions: a practical approach. Oxford University Press, Oxford, United Kingdom.
11. **Card, J. P., M. E. Whealy, A. K. Robbins, and L. W. Enquist.** 1992. Pseudorabies virus envelope glycoprotein gI influences both neurotropism and virulence during infection of the rat visual system. J. Virol. **66:**3032–3041.
12. **Ch'ng, T. H., and L. W. Enquist.** 2005. Neuron-to-cell spread of pseudorabies virus in a compartmented neuronal culture system. J. Virol. **79:**10875–10889.
13. **Ch'ng, T. H., E. A. Flood, and L. W. Enquist.** 2005. Culturing primary and transformed neuronal cells for studying pseudorabies virus infection. Methods Mol. Biol. **292:**299–316.
14. **Ch'ng, T. H., P. G. Spear, F. Struyf, and L. W. Enquist.** 2007. Glycoprotein D-independent spread of pseudorabies virus infection in cultured peripheral nervous system neurons in a compartmented system. J. Virol. **81:**10742–10757.
15. **Ciarlet, M., S. E. Crawford, and M. K. Estes.** 2001. Differential infection of polarized epithelial cell lines by sialic acid-dependent and sialic acid-independent rotavirus strains. J. Virol. **75:**11834–11850.
16. **Da Costa, X. J., C. A. Jones, and D. M. Knipe.** 1999. Immunization against genital herpes with a vaccine virus that has defects in productive and latent infection. Proc. Natl. Acad. Sci. USA **96:**6994–6998.
17. **Desai, P., N. A. DeLuca, and S. Person.** 1998. Herpes simplex virus type 1 VP26 is not essential for replication in cell culture but influences production of infectious virus in the nervous system of infected mice. Virology **247:**115–124.
18. **Dingwell, K. S., C. R. Brunetti, R. L. Hendricks, Q. Tang, M. Tang, A. J. Rainbow, and D. C. Johnson.** 1994. Herpes simplex virus glycoproteins E and I facilitate cell-to-cell spread in vivo and across junctions of cultured cells. J. Virol. **68:**834–845.
19. **Dingwell, K. S., L. C. Doering, and D. C. Johnson.** 1995. Glycoproteins E and I facilitate neuron-to-neuron spread of herpes simplex virus. J. Virol. **69:**7087–7098.
20. **Dingwell, K. S., and D. C. Johnson.** 1998. The herpes simplex virus gE-gI complex facilitates cell-to-cell spread and binds to components of cell junctions. J. Virol. **72:**8933–8942.
21. **Dohner, K., K. Radtke, S. Schmidt, and B. Sodeik.** 2006. Eclipse phase of herpes simplex virus type 1 infection: efficient dynein-mediated capsid transport without the small capsid protein VP26. J. Virol. **80:**8211–8224.
22. **Dohner, K., A. Wolfstein, U. Prank, C. Echeverri, D. Dujardin, R. Vallee, and B. Sodeik.** 2002. Function of dynein and dynactin in herpes simplex virus capsid transport. Mol. Biol. Cell **13:**2795–2809.
23. **Douglas, M. W., R. J. Diefenbach, F. L. Homa, M. Miranda-Saksena, F. J. Rixon, V. Vittone, K. Byth, and A. L. Cunningham.** 2004. Herpes simplex virus type 1 capsid protein VP26 interacts with dynein light chains RP3 and

Tctex1 and plays a role in retrograde cellular transport. J. Biol. Chem. **279:**28522–28530.

24. **Farnsworth, A., K. Goldsmith, and D. C. Johnson.** 2003. Herpes simplex virus glycoproteins gD and gE/gI serve essential but redundant functions during acquisition of the virion envelope in the cytoplasm. J. Virol. **77:**8481–8494.
25. **Farnsworth, A., and D. C. Johnson.** 2006. Herpes simplex virus gE/gI must accumulate in the *trans*-Golgi network at early times and then redistribute to cell junctions to promote cell-cell spread. J. Virol. **80:**3167–3179.
26. **Fehler, F., J. M. Herrmann, A. Saalmuller, T. C. Mettenleiter, and G. M. Keil.** 1992. Glycoprotein IV of bovine herpesvirus 1-expressing cell line complements and rescues a conditionally lethal viral mutant. J. Virol. **66:** 831–839.
27. **Frank, I., and H. M. Friedman.** 1989. A novel function of the herpes simplex virus type 1 Fc receptor: participation in bipolar bridging of antiviral immunoglobulin G. J. Virol. **63:**4479–4488.
28. **Granzow, H., B. G. Klupp, and T. C. Mettenleiter.** 2005. Entry of pseudorabies virus: an immunogold-labeling study. J. Virol. **79:**3200–3205.
29. **Griffiths, A., S. Renfrey, and T. Minson.** 1998. Glycoprotein C-deficient mutants of two strains of herpes simplex virus type 1 exhibit unaltered adsorption characteristics on polarized or non-polarized cells. J. Gen. Virol. **79:**807–812.
30. **Huber, M. T., T. W. Wisner, N. R. Hegde, K. A. Goldsmith, D. A. Rauch, R. J. Roller, C. Krummenacher, R. J. Eisenberg, G. H. Cohen, and D. C. Johnson.** 2001. Herpes simplex virus with highly reduced gD levels can efficiently enter and spread between human keratinocytes. J. Virol. **75:**10309–10318.
31. **Jacobs, L., W. A. Mulder, J. T. Van Oirschot, A. L. Gielkens, and T. G. Kimman.** 1993. Deleting two amino acids in glycoprotein gI of pseudorabies virus decreases virulence and neurotropism for pigs, but does not affect immunogenicity. J. Gen. Virol. **74:**2201–2206.
32. **Johnson, D. C., M. C. Frame, M. W. Ligas, A. M. Cross, and N. D. Stow.** 1988. Herpes simplex virus immunoglobulin G Fc receptor activity depends on a complex of two viral glycoproteins, gE and gI. J. Virol. **62:**1347–1354.
33. **Johnson, D. C., M. Webb, T. W. Wisner, and C. Brunetti.** 2001. Herpes simplex virus gE/gI sorts nascent virions to epithelial cell junctions, promoting virus spread. J. Virol. **75:**821–833.
34. **Kristensson, K., E. Lycke, M. Roytta, B. Svennerholm, and A. Vahlne.** 1986. Neuritic transport of herpes simplex virus in rat sensory neurons in vitro. Effects of substances interacting with microtubular function and axonal flow [nocodazole, taxol and erythro-9-3-(2-hydroxynonyl)adenine]. J. Gen. Virol. **67:**2023–2028.
35. **Lemaire, M., F. Schynts, G. Meyer, J. P. Georgin, E. Baranowski, A. Gabriel, C. Ros, S. Belak, and E. Thiry.** 2001. Latency and reactivation of a glycoprotein E negative bovine herpesvirus type 1 vaccine: influence of virus load and effect of specific maternal antibodies. Vaccine **19:**4795–4804.
36. **Ligas, M. W., and D. C. Johnson.** 1988. A herpes simplex virus mutant in which glycoprotein D sequences are replaced by beta-galactosidase sequences binds to but is unable to penetrate into cells. J. Virol. **62:**1486–1494.
37. **Loret, S., G. Guay, and R. Lippe.** 2008. Comprehensive characterization of extracellular herpes simplex virus type 1 virions. J. Virol. **82:**8605–8618.
38. **Luxton, G. W., S. Haverlock, K. E. Coller, S. E. Antinone, A. Pincetic, and G. A. Smith.** 2005. Targeting of herpesvirus capsid transport in axons is coupled to association with specific sets of tegument proteins. Proc. Natl. Acad. Sci. USA **102:**5832–5837.
39. **Martinez-Moreno, M., I. Navarro-Lerida, F. Roncal, J. P. Albar, C. Alonso, F. Gavilanes, and I. Rodriguez-Crespo.** 2003. Recognition of novel viral sequences that associate with the dynein light chain LC8 identified through a pepscan technique. FEBS Lett. **544:**262–267.
40. **Nagashunmugam, T., J. Lubinski, L. Wang, L. T. Goldstein, B. S. Weeks, P. Sundaresan, E. H. Kang, G. Dubin, and H. M. Friedman.** 1998. In vivo immune evasion mediated by the herpes simplex virus type 1 immunoglobulin G Fc receptor. J. Virol. **72:**5351–5359.
41. **Polcicova, K., K. Goldsmith, B. L. Rainish, T. W. Wisner, and D. C. Johnson.** 2005. The extracellular domain of herpes simplex virus gE is indispensable for efficient cell-to-cell spread: evidence for gE/gI receptors. J. Virol. **79:** 11990–12001.
42. **Rauh, I., and T. C. Mettenleiter.** 1991. Pseudorabies virus glycoproteins gII and gp50 are essential for virus penetration. J. Virol. **65:**5348–5356.
43. **Saksena, M. M., H. Wakisaka, B. Tijono, R. A. Boadle, F. Rixon, H. Takahashi, and A. L. Cunningham.** 2006. Herpes simplex virus type 1 accumulation, envelopment, and exit in growth cones and varicosities in mid-distal regions of axons. J. Virol. **80:**3592–3606.
44. **Saldanha, C. E., J. Lubinski, C. Martin, T. Nagashunmugam, L. Wang, H. van Der Keyl, R. Tal-Singer, and H. M. Friedman.** 2000. Herpes simplex virus type 1 glycoprotein E domains involved in virus spread and disease. J. Virol. **74:**6712–6719.
45. **Samuel, M. A., H. Wang, V. Siddharthan, J. D. Morrey, and M. S. Diamond.** 2007. Axonal transport mediates West Nile virus entry into the central nervous system and induces acute flaccid paralysis. Proc. Natl. Acad. Sci. USA **104:**17140–17145.
46. **Smeraski, C. A., P. J. Sollars, M. D. Ogilvie, L. W. Enquist, and G. E. Pickard.** 2004. Suprachiasmatic nucleus input to autonomic circuits identified by retrograde transsynaptic transport of pseudorabies virus from the eye. J. Comp. Neurol. **471:**298–313.
47. **Smith, G. A., S. P. Gross, and L. W. Enquist.** 2001. Herpesviruses use bidirectional fast-axonal transport to spread in sensory neurons. Proc. Natl. Acad. Sci. USA **98:**3466–3470.
48. **Smith, G. A., L. Pomeranz, S. P. Gross, and L. W. Enquist.** 2004. Local modulation of plus-end transport targets herpesvirus entry and egress in sensory axons. Proc. Natl. Acad. Sci. USA **101:**16034–16039.
49. **Sodeik, B., M. W. Ebersold, and A. Helenius.** 1997. Microtubule-mediated transport of incoming herpes simplex virus 1 capsids to the nucleus. J. Cell Biol. **136:**1007–1021.
50. **Sugimoto, K., M. Uema, H. Sagara, and Y. Kawaguchi.** 2008. Visualization of the assembly of capsid, tegument and envelope proteins in modified TGN with triple-fluorescent HSV-1, abstr. 4.37. 33rd Int. Herpesvirus Workshop, Estoril, Portugal.
51. **Tirabassi, R. S., R. A. Townley, M. G. Eldridge, and L. W. Enquist.** 1997. Characterization of pseudorabies virus mutants expressing carboxy-terminal truncations of gE: evidence for envelope incorporation, virulence, and neurotropism domains. J. Virol. **71:**6455–6464.
52. **Topp, K. S., L. B. Meade, and J. H. LaVail.** 1994. Microtubule polarity in the peripheral processes of trigeminal ganglion cells: relevance for the retrograde transport of herpes simplex virus. J. Neurosci. **14:**318–325.
53. **Trapp, S., N. Osterrieder, G. M. Keil, and M. Beer.** 2003. Mutagenesis of a bovine herpesvirus type 1 genome cloned as an infectious bacterial artificial chromosome: analysis of glycoprotein E and G double deletion mutants. J. Gen. Virol. **84:**301–306.
54. **Tyborowska, J., K. Bienkowska-Szewczyk, M. Rychlowski, J. T. Van Oirschot, and F. A. Rijsewijk.** 2000. The extracellular part of glycoprotein E of bovine herpesvirus 1 is sufficient for complex formation with glycoprotein I but not for cell-to-cell spread. Arch. Virol. **145:**333–351.
55. **van Engelenburg, F. A., M. J. Kaashoek, J. T. van Oirschot, and F. A. Rijsewijk.** 1995. A glycoprotein E deletion mutant of bovine herpesvirus 1 infects the same limited number of tissues in calves as wild-type virus, but for a shorter period. J. Gen. Virol. **76:**2387–2392.
56. **Wang, F., W. Tang, H. M. McGraw, J. Bennett, L. W. Enquist, and H. M. Friedman.** 2005. Herpes simplex virus type 1 glycoprotein E is required for axonal localization of capsid, tegument, and membrane glycoproteins. J. Virol. **79:**13362–13372.
57. **Weeks, B. S., and H. M. Friedman.** 1997. Laminin reduces HSV-1 spread from cell to cell in human keratinocyte cultures. Biochem. Biophys. Res. Commun. **230:**466–469.
58. **Weeks, B. S., P. Sundaresan, T. Nagashunmugam, E. Kang, and H. M. Friedman.** 1997. The herpes simplex virus-1 glycoprotein E (gE) mediates IgG binding and cell-to-cell spread through distinct gE domains. Biochem. Biophys. Res. Commun. **235:**31–35.
59. **Wisner, T., C. Brunetti, K. Dingwell, and D. C. Johnson.** 2000. The extracellular domain of herpes simplex virus gE is sufficient for accumulation at cell junctions but not for cell-to-cell spread. J. Virol. **74:**2278–2287.
60. **Ye, G. J., and B. Roizman.** 2000. The essential protein encoded by the UL31 gene of herpes simplex virus 1 depends for its stability on the presence of UL34 protein. Proc. Natl. Acad. Sci. USA **97:**11002–11007.